Pegylation: A Method for Assessing Topological Accessibilities in Kv1.3[†]

Jianli Lu and Carol Deutsch*

Department of Physiology, University of Pennsylvania, Philadelphia, Pennsylvania 19104-6085

Received April 16, 2001; Revised Manuscript Received August 31, 2001

ABSTRACT: Each subunit of a voltage-gated potassium channel (Kv) contains six putative transmembrane segments, S1−S6, and a cytosolic N-terminal recognition domain, T1. Although it is well-established that Kv channels are tetrameric structures, the protein−protein, protein−lipid, and protein−aqueous interfaces are not precisely mapped. The topological accessibility of specific amino acids may help to identify these border residues. Toward this end, a variant of the substituted-cysteine-accessibility method that relies on mass-labeling of accessible SH groups with a large SH reagent, methoxy-polyethylene glycol maleimide, and gel shift assay has been used. *Pegylation* of full-length Kv1.3, as well as Kv1.3 fragments, integrated into microsomal membranes, allows topological characterization of the 12 native cysteines (C1−C12), as well as cysteines engineered into a T1−T1 interface. Cysteines engineered into the T1−T1 interface had lower rates of pegylation than cytosolic-facing cysteines, namely, C5 in the T1 domain and C10−C12 in the C terminus.

Voltage-gated potassium (Kv) channels are tetrameric structures (*1*, *2*) embedded in a lipid bilayer. Potential inter- and intrasubunit contact sites for a prokaryotic K^+ channel from *Streptomyces lividans* (KcsA) (*3*, *4*) and for eukaryotic Kv channels (*5*−*8*) have been identified. Additionally, intersubunit interactions between core transmembrane segments have been implicated by several studies of NH_2-terminally deleted Kv channels (*9*−*15*). Residues directly contributing to subunit−subunit interactions, or intrasubunit interactions, will be at protein−protein interfaces. The remaining residues will be either at protein−lipid interfaces or at protein−aqueous interfaces, including the cytoplasmic and extracellular membrane borders. One strategy for identifying Kv channel residues at protein−protein interfaces is alanine or tryptophan scanning (*16*−*18*). Identifying residues at either protein−lipid or protein−aqueous interfaces requires a different approach.

As an approach to interface identification, we have developed a strategy that is a variant of the substituted-cysteine-accessibility method (*19*−*21*). Our strategy relies on the mass-tagging of accessible SH groups with a large SH reagent, methoxy-polyethylene glycol maleimide (MAL-PEG, MW 5000; Shearwater, Inc). MAL-PEG reagent has the following advantageous properties for our purpose. It does not cross membranes even upon incubation at 4 °C for >24 h at high concentration. For every SH group, MAL-PEG adds a PEG molecule, which shifts the apparent molecular weight of the parent protein by ≥10 kDa. The adduct is stable in water under reducing conditions because the newly formed bond is a covalent C−S bond, is stable in detergents including SDS, and is relatively specific for SH groups (maleimides react ∼1000 times more rapidly with SH groups than with amino groups at neutral pH). Its limitations are that the number of SH groups that can simultaneously be assayed depends on the parent protein molecular weight (up to 9−10 cysteines in proteins in the molecular weight range from 10 to 200 kDa), and reaction rates are slow compared with smaller maleimides.

In membrane-integrated Kv1.3, cysteines located at protein−aqueous interfaces facing the impermeant MAL-PEG will be labeled. Cysteines located at the protein−lipid interface in the membrane and those buried at protein−protein interfaces will not be labeled unless first exposed using an appropriate detergent. Cytoplasmic-facing cysteines can be distinguished from lumenal (extracellular)-facing cysteines by using (i) small, hydrophilic, impermeant or (ii) small, membrane-permeant SH reagents, respectively, in the absence of detergent, to block available cysteines prior to pegylation. The covalently bound blockers have too small a molecular weight to be detected on SDS−PAGE gels. In this paper we have used *pegylation* to identify available SH groups in full-length Kv1.3, as well as in Kv1.3 fragments, to determine their respective orientation and topology in microsomal (endoplasmic reticulum, ER) membranes. Our results suggest that pegylation will be a powerful tool in the arsenal of techniques used to explore the topology of membrane proteins. A preliminary report of this work has appeared previously (*22*).

MATERIALS AND METHODS

Recombinant DNA Techniques. Standard methods of plasmid DNA preparation, restriction enzyme analysis, agarose gel electrophoresis, and bacterial transformation were used. All isolated fragments were purified with Geneclean (Bio 101 Inc., La Jolla, CA), recircularized using T4 DNA ligase, and then used to transform DH5α or JM 109 competent cells (Promega, Madison, WI). The nucleotide sequences of all mutants were confirmed by restriction enzyme analysis or by automated cycle sequencing per-

[†] Supported by National Institutes of Health Grant GM 52302.

* Corresponding author [fax (215) 573-5851; e-mail cjd@mail.med.upenn.edu; telephone (215) 898-8014].

10.1021/bi0107647 CCC: $20.00
Published on Web 10/09/2001

formed by the DNA Sequencing Facility at the School of Medicine, University of Pennsylvania, on an ABI 377 sequencer using Big dye terminator chemistry (ABI).

Plasmid Constructs. All mutant DNAs were sequenced in the region of the mutation. Additionally, for cysteine-free and engineered R118C/D126C, the entire open reading frame of the gene was sequenced. pSP/Kv1.3(T1$^-$) was generated by cutting pSP vector with *Nco*I/*Xba*I, cutting pGEM/Kv1.3 (*13*) with *Nco*I/*Spe*I, and ligating the vector and the insert. Kv1.3(T1$^-$)/C7$^-$ was generated from the pSP/Kv1.3(T1$^-$) template using the QuikChange site-directed mutagenesis kit (Stratagene, La Jolla, CA) to make the C250S mutation site. Throughout the text S1−S6 refers to the transmembrane segments 1−6, respectively, in Kv1.3. Clones of pSP/S1 and pSP/S1−S2−S3 were generated using Kv1.3(T1$^-$) as a template, a sense oligonucleotide starting at SP6, and the antisense oligonucleotide for S1 and S1−S2−S3, respectively. Clone S5−S6−C-terminus was generated by ligation of a 0.5 kb fragment obtained from *dra*III/*Bam*HI digestion of pSP/Kv1.3 into a *dra*III/*Bam*HI-digested pSP/S5−S6−C-prolactin (*23*). pSP/Kv1.3/cysteine-free (referred to as C-free in the text and figures) was generated by removal of all 12 native cysteines from the pSP/Kv1.3 template using the QuikChange site-directed mutagenesis kit (Stratagene). The mutations are, in order from the first cysteine in the sequence (C1) to the last (C12), C26S, C31S, C49S, C50S, C71S, C200V, C250S, C265S, C412A, C453S, C504S, and C513S. pSP/Kv1.3/C1−C8$^-$/C9$^+$/C10−C12$^-$ is referred to in the text and figures as C9$^+$. pSP/Kv1.3/C1−C4$^-$/C5$^+$/C6−C9$^-$/C10−C12$^+$ is referred to as C5$^+$/C10−C12$^+$ in the text and figures and contains mutated C6−C9 (C200V, C250S, C265S, and C412A) as well as mutated C1−C4 (C26S, C31S, C49S, and C50S).

pSP/Kv1.3/C1−C5$^-$/C6−C12$^+$/R118C/D126C was generated by ligating a fragment (0.74 kb) from *Nco*I/*Bst*EII digestion of pSP/Kv1.3 into *Nco*I/*Bst*EII-digested pSP/Kv1.3/C1−C8$^-$/C9$^+$/C10−C12$^-$. pSP/Kv1.3/C1−C5$^-$/C6−C9$^+$/C10−C12$^-$/R118C/D126C/Flag (referred to as R118C/D126C in the text and figures) was generated by ligating a *Pst*I/*Eco*RI-digested fragment from pSP/Kv1.3/C1−C5$^-$/C6−C12$^+$/R118C/D126C into pSP/Kv1.3/C1−C8$^-$/C9$^+$/C10−C12$^-$/Flag, which was generated from the pSP/Kv1.3/cysteine-free/Flag template using the QuikChange site-directed mutagenesis kit. pSP/Kv1.3/C1−C5$^-$/C6−C9$^+$/C10−C12$^-$/R62C/E64C/Flag (referred to as R62C/E64C in the text and figures) was generated by ligation of a fragment obtained from *Pst*I/*Eco*RI digestion of pSP/Kv1.3/C1−C5$^-$/C6−C12$^+$/R62C/E64C into pSP/Kv1.3/C1−C8$^-$/C9$^+$/C10−C12$^-$/Flag, made as described above from the pSP/Kv1.3/cysteine-free/Flag template. pSP/Kv1.3/D126C and pSP/Kv1.3/R118C, referred to as D126C and R118C, respectively, in the text and legends, were each made from the cysteine-free template using the QuikChange site-directed mutagenesis kit.

In Vitro Translation. Capped cRNA was synthesized in vitro from linearized templates using Sp6 RNA polymerase (Promega). Proteins were translated in vitro with [^{35}S]-methionine (2 μL/25 μL translation mixture; ~10 μCi/μL express, Dupont/NEN Research Products, Boston, MA) for 120 min at 30 °C in the presence of canine microsomal membranes in rabbit reticulocyte lysate according to the *Promega Protocol and Application Guide*.

Pegylation Assays. Translation product (5−10 μL) was centrifuged through a sucrose cushion (100 μL; 0.5 M sucrose, 100 mM KCl, 5 mM $MgCl_2$, 50 mM Hepes, 1 mM DTT, pH 7.5) for 5 min at 55000 rpm at 4 °C to isolate only membrane-integrated protein. The pellet was solubilized for 1 h in phosphate-buffered saline (PBS; 50 μL) containing 137 mM NaCl, 1.2 mM KH_2PO_4, 15.3 mM Na_2HPO_4, 2.7 mM KCl, 2 mM EDTA, 1 mM DTT, pH 6.5−7.3, and either no detergent or 1% sodium dodecyl sulfate (SDS). When SDS was used, the pellet was solubilized at room temperature; when no detergent was used, the samples were solubilized at 0−4 °C. Effective resuspension of membrane vesicles in the absence of detergent required careful (avoid bubble formation), repetitive pipetting (>100 times). Resuspended protein was diluted with 50 μL of PBS containing 2 mM EDTA, 40 mM MAL-PEG, and no DTT to give a final MAL-PEG concentration of 20 mM, incubated at 4 °C for 15 min or 3, 6, or 16−19 h, and analyzed by SDS−PAGE or LDS−NUPAGE. For some constructs, shorter incubation times at 4 °C and 20 mM reagent were insufficient to label all cysteines. Samples were prepared for SDS−PAGE by adding 100 μL of loading buffer containing 7.2% SDS, 2 M Tris base, 34% glycerol, 171 mM DTT, and 0.85% bromophenol blue. When precast NUPAGE gels were used, we added 40 μL of NUPAGE loading buffer (4× stock) and 16 μL of NUPAGE reducing agent (10× stock) to 100 μL samples. MAL-PEG was stored as the dry powder at −20 °C and made fresh just prior to each experiment. In some cases, small (non-mass-detectable) blocking agents, 4-acetamido-4-maleimidylstilbene-2,2-disulfonic acid (AMS) and *N*-ethylmaleimide (NEM), were used prior to the sucrose cushion step at the concentrations and times indicated under Results. AMS and NEM were stored as the dry powder at −20 °C and made fresh just prior to each experiment. The kinetics of pegylation are pH-dependent, the reaction being faster at alkaline pH. However, the specificity is less stringent and, consequently, the background higher, at alkaline pH. Therefore, a balance between these two conditions must be chosen for each construct. In general, for constructs containing zero to two cysteines, a pH of 6.5−6.8 was used; for constructs containing three or more cysteines, a pH of 7.0−7.3 was used.

The rate constants for pegylation of select residues were determined. C5 in a Kv1.3 construct that contains only this exposed cysteine (*5*−*7*) is 8 M^{-1} s^{-1} at pH 7.0 and 4 °C (137 mM NaCl, 1.2 mM KH_2PO_4, 15.3 mM Na_2HPO_4, 2.7 mM KCl, and 2 mM EDTA). The rate constant for NEM labeling of C5 is 126 M^{-1} s^{-1} at pH 7.0 and 4 °C. Under similar conditions, the rate constant for pegylation of C12 is 170 M^{-1} s^{-1}. Pegylation in 1% SDS of C9 in a Kv1.3 construct that contains only this cysteine is complete within 10−15 min at pH 7.0 and 4 °C (137 mM NaCl, 1.2 mM KH_2PO_4, 15.3 mM Na_2HPO_4, 2.7 mM KCl, and 2 mM EDTA) using 1 mM MAL-PEG, thus giving a rate constant of ≥8 M^{-1} s^{-1}. Pegylation of β-mercaptoethanol is complete (4,4′-dithiodipyridine absorbance assay at 324 nm (*24*)) within 5 s at pH 8.0 and 4 °C (0.1 M borate buffer and 5 mM EDTA) using 2 mM MAL-PEG, thus giving a rate constant ≥500 M^{-1} s^{-1}.

Analysis of Pegylation Ladders. For any given construct, the radioactive bands in SDS−PAGE of protein incubated with MAL-PEG were quantitated using PhosphorImaging

and the data analyzed as follows. The fraction of total protein, $F(i)$, with a given number of SH pegylated per protein molecule, i, was calculated as $F(i) = \text{cpm}(i)/\sum\text{cpm}(i)$, where $i = 0-i_{max}$ and cpm are counts per minute in the ith bin. A statistical comparison between different $F(i)$ distributions was made using a Kolmogorov−Smirnov test (*25*) to yield a p significance value. The average number of pegylated cysteines in each construct is $X = \sum iF(i)$. If each cysteine has the same accessibility and is pegylated independently, then the number of pegylated cysteines will obey a binomial distribution $B(i,N)$, where N is the total number of cysteines in the molecule and the probability of an individual cysteine being pegylated, P, is X/N. P can be used to calculate the binomial distribution, $B(i,N) = [(P)^i(1-P)^{N-i}N!/i!(N-i)!]$. A statistical comparison of the $F(i)$ and $B(i,N)$ distributions was made using a Kolmogorov−Smirnov test. To estimate the fraction of cysteines unpegylated, singly pegylated, or doubly pegylated for the data shown in Figure 8, the following equations were used, respectively: $P_0 = (1-P_R)(1-P_D)$; $P_1 = 1-P_2-P_0$; $P_2 = P_RP_D$, where P_R and P_D are the fractions of singly labeled cysteines for constructs R118C and D126C, respectively (data shown in Figure 9).

Sucrose Gradients. Twenty-five microliters of translation product (containing membranes) was centrifuged through a sucrose cushion (100 μL; 0.5 M sucrose, 100 mM KCl, 5 mM $MgCl_2$, 50 mM Hepes, and 1 mM DTT, pH 7.5) for 5 min at 55000 rpm at 4 °C. The pellet was resuspended in Hepes buffer (200−300 μL) containing 200 mM NaCl, 2 mM EDTA, 1 mM DTT, 20 mM Hepes, pH 8.0−8.4, and 0.05% C_{12}M and kept on ice for 1 h. The solution was centrifuged at 60000 rpm for 60 min and the supernatant loaded on the top of a 5−20% sucrose Hepes buffer gradient column, spun at 36000 rpm in an SW40T rotor for 20 h at 4 °C. Fractions (0.35 mL) were collected and precipitated with trichloroacetic acid and analyzed by SDS−PAGE. The fractional migration was calibrated using molecular weight standards: carbonic anhydrase (MW = 29 kDa), bovine serum albumin (MW = 66 kDa), fumerase (MW = 206 kDa), and catalase (MW = 250 kDa). The Kv1.3 protein distributed in the sucrose gradients represents >90% of the protein in the ER membranes.

Gel Electrophoresis and Fluorography. Electrophoresis was performed on a C.B.S. Scientific gel apparatus using 15% SDS−polyacrylamide gels, depending on the molecular weight of the proteins being assayed. Gels were made according to standard Sigma protocols (Sigma Technical Bulletin MWM-100). SDS in the sampling buffer, running buffer, and gel was 3.6, 0.1, and 0.1%, respectively. Alternatively, some gels were run using the NUPAGE system Bis-Tris 10%, 12%, or gradient 4−12% gels. Gels were soaked in Amplify (Amersham Corp., Arlington Heights, IL) to enhance ^{35}S fluorography, dried, and exposed to Kodak X-AR film at −70 °C. Typical exposure times were 16−30 h. Quantitation of gels was carried out directly using a Molecular Dynamic PhosphorImager (Sunnyvale, CA), which is very sensitive and detects cpm that are not necessarily visualized in autoradiograms exposed for 16−30 h. Thus, some bands, at the level of 5−10% of the protein, are not visible but are detected by PhosphorImaging.

Oocyte Expression and Electrophysiology. Oocytes were isolated from *Xenopus laevis* females (Xenopus I, Michigan) as described previously (*26*). Stage V−VI oocytes were selected and microinjected with 0.05−0.5 ng of cRNA encoding for wild-type or mutant Kv1.3. K^+ currents from cRNA-injected oocytes were measured with a two-microelectrode voltage clamp using an OC-725C oocyte clamp (Warner Instrument Corp., Hamden, CT) after 24−48 h, at which time currents were 2−10 μA. Electrodes (<1 MΩ) contained 3 M KCl. The currents were filtered at 1 kHz. The bath Ringer solution contained 116 mM NaCl, 2 mM KCl, 1.8 mM $CaCl_2$, 2 mM $MgCl_2$, and 5 mM Hepes (pH 7.6). The holding potential was −100 mV. For experiments in which inactivation kinetics were determined, we fit the data at 50 mV using the simplex algorithm (Clampfit, Axon Instruments).

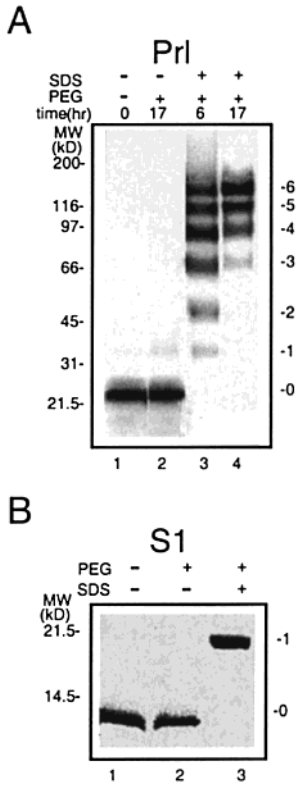

FIGURE 1: Pegylation of Prl and S1. (A) Prl was translated and labeled with [^{35}S]methionine in a rabbit reticulocyte lysate containing microsomal membranes. In the absence of detergent (lanes 1 and 2), pegylation of Prl reflects the *leakiness* of the vesicles to Prl or MAL-PEG. SDS (1%) solubilizes the membrane vesicles, as measured by the absence of radioactivity in the pellet from a high-speed spin of the solubilized vesicles, exposing lumenal Prl to membrane impermeant MAL-PEG (lanes 3 and 4). Pegylation was carried out as described under Materials and Methods for the times indicated. These data are representative of five experiments. (B) S1 was translated, labeled with [^{35}S]methionine, and pegylated, as described for Prl. These data are representative of five identical experiments. For both parts A and B, the numbers to the left of the gels are MW standards (kDa); the numbers to the right indicate unpegylated (0) and multiply pegylated (1−6) protein, respectively.

RESULTS

Verification of the Pegylation Method. To demonstrate the ability of MAL-PEG to stably label proteins generated by in vitro translation in microsomal membrane vesicles, we translated two types of ^{35}S-labeled control proteins and pegylated them with MAL-PEG. The first control protein, bovine preprolactin (Prl; 25 kDa), is a secretory protein with

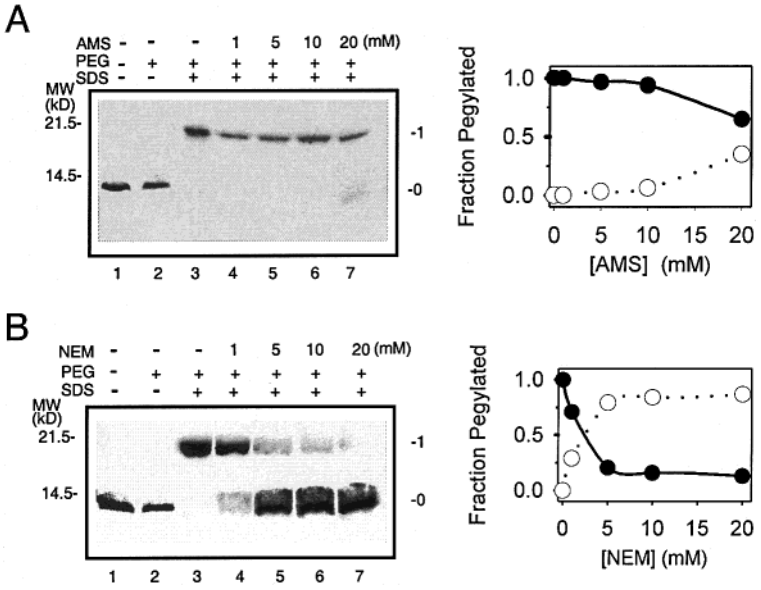

FIGURE 2: Block of S1 pegylation by AMS and NEM. S1 was translated, pretreated with either AMS (A), NEM (B), or no blocker for 2 h at 4 °C, and then pegylated either in the absence of detergent or in SDS. In the left panels of (A) and (B), the numbers to the left of the gel are MW standards (kDa); the numbers to the right indicate unpegylated (0) and singly pegylated (1) protein, respectively. In the right panels of (A) and (B), pegylation was quantitated by PhosphorImager analysis of level 0 and 1 bands in each lane and plotted as fraction of protein pegylated for each blocker concentration. Solid circles represent the fraction pegylated; open circles represent the fraction unpegylated. The gels shown in (A) are 12% LDS−NUPAGE gels with MES running buffer; those shown in (B) are 12% LDS−NUPAGE gels with MOPS running buffer.

six internal disulfide-linked cysteines. We have shown that in our experimental in vitro system, 90−95% of this protein is located in the aqueous compartment of the vesicle lumen (*23*). The second control protein, S1, is the first transmembrane segment of Kv1.3. S1, which is integrated into the vesicle membrane and oriented with its C terminus in the lumen (*23*, *27*), contains one cysteine, located at the C terminus of the construct. After translation, both Prl and S1 should be protected from pegylation because the available SH groups are in, or close to, the lumen. However, detergent treatment solubilizes the membrane and should permit labeling of available SH groups. Figure 1 shows this was indeed the case.

Prl was translated in the presence of DTT to ensure that all six cysteines were available for subsequent pegylation. Translated Prl, in the absence of detergent, gave a single band in the absence or presence of MAL-PEG (Figure 1A, lanes 1 and 2). Pegylation did not occur, indicating that the membranes were not leaky to either Prl or MAL-PEG. On the other hand, Prl derived from SDS-solubilized vesicles gave a ladder of bands (lanes 3) shifted from the unpegylated parent (lanes 1 and 2), which is indicated by the number "0" on the right of the gel. No unpegylated Prl remained after treatment with MAL-PEG. Numbers 1−6 indicate protein labeled with one to six PEG molecules, respectively. All Prl had at least one pegylated cysteine in the presence of detergent. The pegylation conditions are reducing, and therefore all six SH groups were available to form PEG adducts.[1] When oxidizing translation conditions (2 mM oxidized glutathione) were used to translate Prl, subsequent treatment with MAL-PEG gave only unpegylated Prl (data not shown).

Translated S1, in the absence of detergent, gave a single band at ~9 kDa in the absence and presence (lanes 1 and 2, respectively, in Figure 1B) of MAL-PEG. Pegylation did not occur. However, S1 derived from SDS-solubilized vesicles also gave one band after treatment with MAL-PEG (lane 3), but the molecular weight was ~22 kDa, indicating that all of the S1 protein was pegylated with one PEG per protein molecule. These results are consistent with the experimentally determined topology of S1 (*23*), which locates its one cysteine in the lumen.

We also used these control proteins, Prl and S1, to determine optimal conditions for non-mass-tagging SH reagents that were included in our assays prior to pegylation. The purpose of these SH reagents was to distinguish cytoplasmic-facing cysteines from lumenal (extracellular)-facing cysteines, using 4-acetamido-4-maleimidylstilbene-2,2-disulfonic acid (AMS), a charged membrane-impermeant maleimide, and *N*-ethylmaleimide (NEM), an uncharged membrane-permeant blocker, respectively. In the absence of detergent, these small SH reagents will react irreversibly with available cysteines prior to pegylation, and the covalently bound blockers have too small a molecular weight to be detected on Bis-Tris gels. Therefore, in our experiments we pretreated intact vesicles with AMS or NEM in the absence of detergent and then solubilized and pegylated them. AMS should react with only cytosolic SH groups, and NEM should react with both cytosolic and lumenal SH groups. Appropriate conditions were defined in our microsomal membrane preparation as the minimum time and concentration of AMS required to completely label cytosolic, but not lumenal, SH groups, and as the minimum time and concentration of NEM required to ensure labeling of all available cytosolic and

[1] The hydrodynamic properties of MAL-PEG cause it to run with slower mobility on LDS−NUPAGE gels, i.e., at 10−15 kDa above the molecular weight of the parent protein. Moreover, addition of multiple MAL-PEG molecules to a protein results in shielding of some of the charge on the protein, and therefore the gel mobilities of the multi-PEG protein adduct are not linear with the number of MAL-PEG per protein.

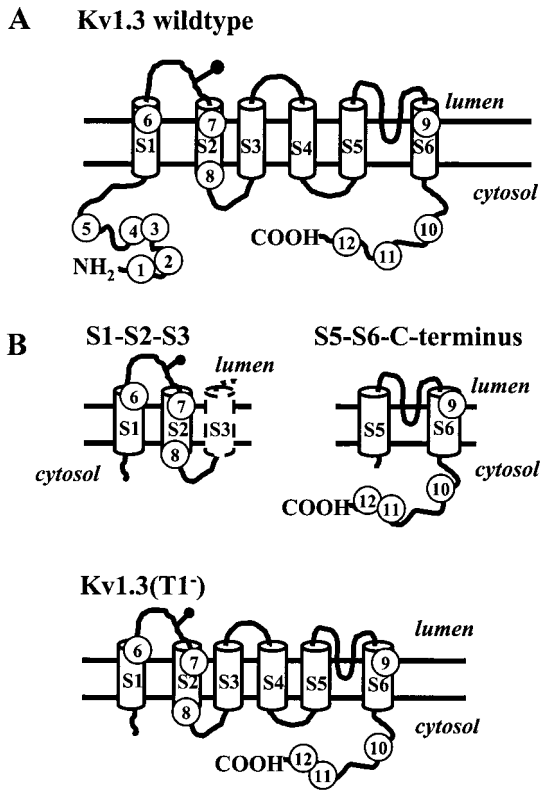

FIGURE 3: Topological representations of Kv1.3 proteins in ER membranes. (A) Topology of full-length wild-type Kv1.3 in the ER membrane, according to ref *23*. Twelve native cysteines are in the NH_2 terminus (C1−C5), S1 (C6), S2 (C7, C8), S6 (C9), and the C terminus (C10−C12), indicated by encircled C1−C12. (B) Topology of fragments S1−S2−S3, S5−S6−C-terminus, and Kv1.3(T1$^-$) in the ER membrane, according to ref *23*. They contain, respectively, three, four, and seven native cysteines, as indicted. Glycosylation is indicated by a ball-and-stick representation and is present in wild-type Kv1.3, S1−S2−S3, and Kv1.3(T1$^-$). S3 is dotted in S1−S2−S3 to reflect the finding that the translocation efficiency of S3 in this construct is <50% (*23*).

lumenal SH groups. With longer times, small, so-called impermeant reagents will cross the membrane and label lumenal SH groups due to time-dependent diffusion and/or increased membrane permeability. Blocking of S1 became significant at AMS concentrations >5 mM (2 h, 4 °C; Figure 2A). For these incubation conditions, the low permeability of the membrane prevents AMS (5 mM) inhibition of the lumenal cysteines. Blockage by 5 mM AMS of cytosolic cysteines is complete within 15−30 min, as shown in Figures 4−7. Blockage by NEM was largest from 1 to 5 mM and maximal (≥80%) at 20 mM within 2 h (Figure 2B; see also Figures 4−7). Therefore, in subsequent experiments we used 5 mM AMS and 20 mM NEM in 15−30 min and 2-h preincubations, respectively.

Pegylation of Kv1.3 Fragments. Because full-length native Kv1.3 (Figure 3) contains 12 cysteines per monomeric subunit, we first applied the pegylation method to native cysteines in simpler Kv1.3 fragments from each end of the Kv1.3 polypeptide, namely, S1−S2−S3 and S5−S6−C-terminus, and then to Kv1.3(T1$^-$), a construct that lacks the first 141 amino acids of the N terminus (*13*, *14*). Figure 3 shows cartoon arrangements of Kv1.3 monomer and Kv1.3 fragments in an endoplasmic reticulum (ER) membrane, consistent with the experimentally determined topology for Kv1.3 and these fragments (*23*). The native cysteines are numbered 1−12 from the N terminus to the C terminus. S1−S2−S3 has three native cysteines (C6, C7, and C8) and is efficiently integrated into microsomal membranes (*23*, *27*). S5−S6−C-terminus has four native cysteines (C9, C10, C11, and C12) and is also efficiently integrated into microsomal membranes with the C terminus in the cytosol (*23*). Kv1.3(T1$^-$) has seven native cysteines (C6−C12) and completely integrates into microsomal membranes and forms functional channels in vivo (*13*, *14*, *23*, *27*).

In our experiments, S1−S2−S3 protein was translated in microsomal membrane vesicles and labeled with [^{35}S]-methionine, incubated with AMS, NEM, or no reagent, and then pelleted through a sucrose cushion to isolate only membrane-integrated protein. Following this treatment, membranes were solubilized either in SDS or in no detergent, then pegylated, and run on SDS−PAGE. Figure 4 shows the results of pegylating S1−S2−S3. S1−S2−S3 contains a consensus site for N-linked glycosylation and therefore appears as a doublet of unglycosylated and glycosylated protein (*27*). In the presence of MAL-PEG and no detergent, S1−S2−S3 was mostly unpegylated (level 0), with a faint band of singly pegylated species (level 1; lane 1). Pegylation of SDS-solubilized S1−S2−S3 gave only pegylated protein, the major bands being doubly and triply pegylated protein (lane 2, Figure 4B; Table 1). Negligible unpegylated protein was detected at level 0. These results indicate that the three native cysteines, C6, C7, and C8, in membrane-integrated S1−S2−S3 are mostly inaccessible from the cytosol.

To determine whether C6, C7, and C8 are accessible from the lumen, we used AMS and NEM prior to pegylation. After AMS pretreatment, only unpegylated S1−S2−S3 was detected in the absence of detergent (lane 3). This suggests that the faint band detected in lane 1 represents a cysteine that can be blocked from the cytosol, perhaps C8 (Figure 3B). In SDS, AMS pretreatment and pegylation gave mostly doubly pegylated protein (level 2 is the darkest band; lane 4, Figure 4B; Table 1), consistent with two of the three native cysteines being located in noncytosolic compartments. We repeated this experiment using NEM, which should react with cysteines in the cytosol and the lumen. Although lipid-facing cysteines could theoretically react with NEM, generation of a reactive thiolate anion in the membrane is rare due to the low dielectric constant of the environment, and the predicted reaction rate would be extremely slow compared to rates with ionized cysteines in an aqueous environment (*28*). Thus, NEM appears to react with SH groups at aqueous interfaces, both cytosolic and lumenal. Preblock with NEM, followed by pegylation, gave only unpegylated S1−S2−S3 in the absence of detergent (doublet at level 0, lane 5) and only 1 pegylated band in SDS (doublet at level 1; lane 6; Table 1). For the experiments shown in Figure 4, the number of pegylated S1−S2−S3 bands was the same after 18 and 50 h of pegylation at 4 °C (data not shown). Although S1−S2−S3 is integrated into microsomal membranes and glycosylated (i.e., translocated; *23*, *27*), some of the cysteines in this fragment do reside in, or visit, aqueous compartments. C8 is accessible to blocker from the cytoplasmic side and can be pegylated, albeit slowly, most likely due to an equilibrium between accessible and inaccessible states at the membrane border. Either C6 or C7 is accessible from the lumenal side of the vesicle and likely resides in an aqueous vestibule. Similar experiments with the S1 segment of Kv1.3

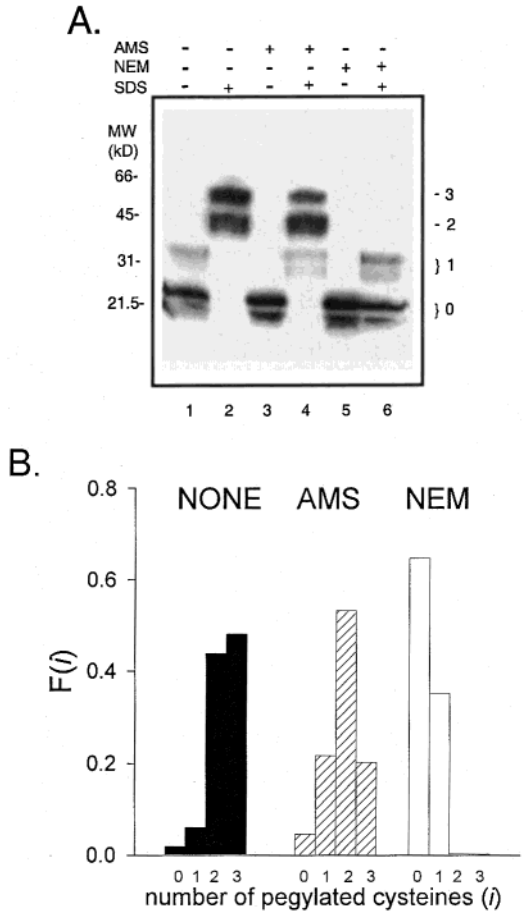

FIGURE 4: Pegylated S1−S2−S3 peptide fragment in membranes. (A) S1−S2−S3 was translated and labeled with [^{35}S]methionine in a rabbit reticulocyte lysate system containing microsomal membranes, incubated with either no blocking reagent (lanes 1 and 2), AMS (5 mM, lanes 3 and 4), or NEM (20 mM, lanes 5 and 6), and then centrifuged through a sucrose cushion. The vesicles were resuspended in either no detergent (lanes 1, 3, and 5) or 1% SDS (lanes 2, 4, and 6), and pegylated. All steps after translation were done at 4 °C. The gels are standard Bio-Rad 15% Tris−glycine gels. The numbers to the left of the gels are MW standards (kDa); the "0, 1, 2, 3" on the right indicate unpegylated, singly, doubly, and triply pegylated protein, respectively. Unpegylated S1−S2−S3 is a doublet of unglycosylated and glycosylated protein (*14*, *27*) but appears as a single broad band at higher molecular weights (>∼40 kDa). These data are representative of five experiments. (B) Fraction of S1−S2−S3 protein pegylated in 1% SDS with the indicated number of MAL-PEG per translated S1−S2−S3 pre-blocked with no reagent (black), AMS (hatched), or NEM (white). The fractions of unpegylated, singly, doubly, and triply pegylated protein were calculated as $F(i) = \text{cpm}(i)/\sum\text{cpm}(i)$, $i = 0-i_{max}$), where i is the number of SH pegylated per protein molecule and cpm(i) is the number of counts per minute in the ith bin. The distribution histograms are significantly different for AMS or NEM pretreatment compared to control (no pretreatment) ($p < 0.001$ and $p < 0.001$, respectively, Komogorov−Smirnov test). The fractional distribution of pegylated S1−S2−S3 in SDS is significantly different from binomality ($p < 0.001$, Komogorov−Smirnov test).

(above, Figure 2) indicate that C6 resides at a protein−aqueous interface in the lumen (Figure 3B).

In summary, the most likely tentative interface assignments for native cysteines in S1−S2−S3 are that C6 and C8 are on opposite sides of the membrane at protein−aqueous interfaces. C7 is inaccessible in the absence of detergent and may be at a protein−protein or protein−lipid interface. These results indicate that S1 and S2 each span the membrane,

Table 1[a]

construct	detergent	blocker	*n* 1	2	3	4	5	6	7
S1−S2−S3			1.0	**[b]	**				
		AMS	**	**	**				
		NEM	**	**	**				
	SDS		0.06	0.45	0.49				
		AMS	0.23	0.56	0.21				
		NEM	1.0	**	**				
S5−S6−C-terminus			0.36	0.32	0.32	**			
		AMS	1.0	**	**	**			
		NEM	1.0	**	**	**			
	SDS		0.15	0.17	0.32	0.36			
		AMS	1.0	**	**	**			
		NEM	**	**	**	**			
Kv1.3(T1$^-$)			0.11	0.22	0.49	0.19	**	**	**
		AMS	1.0	**	**	**	**	**	**
		NEM	**	**	**	**	**	**	**
	SDS		0.02	0.04	0.07	0.11	0.16	0.28	0.33
		AMS	0.28	0.57	0.15	**	**	**	**
		NEM	1.0	**	**	**	**	**	**
Kv1.3(T1$^-$)C7$^-$			0.21	0.24	0.31	0.24	**	**	**
		AMS	**	**	**	**	**	**	**
		NEM	**	**	**	**	**	**	**
	SDS		0.03	0.05	0.09	0.15	0.29	0.40	**
		AMS	0.87	0.13	**	**	**	**	**
		NEM	1.0	**	**	**	**	**	**
C5$^+$/C10−C12$^+$			0.15	0.24	0.30	0.32			
		AMS	1.0	**	**	**			
		NEM	1.0	**	**	**			
	SDS		0.04	0.18	0.35	0.44			
		AMS	1.0	**	**	**			
		NEM	1.0	**	**	**			

[a] Data were obtained by PhosphorImager detection of the gel, not necessarily visible in a 16−30 h exposed autoradiogram. Each entry is the fraction of pegylated protein with n pegylated cysteines, calculated as $F(n) = \text{cpm}(n)/\sum\text{cpm}(n)$, where $n = 1$ to n_{max}. [b] Double asterisks indicate cpm are less than background cpm.

similar to their proposed topology in the full-length channel. This has been confirmed using a complementary reporter method (*23*) and glycosylation assays (*14*, *27*), which show that the C and N termini, respectively, of S1 and S2 are each efficiently translocated across the membrane.

S5−S6−C-terminus protein was similarly pegylated, and the results are shown in Figure 5A,B. In the presence of MAL-PEG and no detergent, no unpegylated protein at level 0 was detected (lane 1). Approximately one-third of the protein is the triply pegylated protein (Figure 5B; Table 1). These results indicate that the three native C-terminal cysteines C10−C12 in membrane-integrated S5−S6−C-terminus are mostly accessible from the cytosol. Pegylation of the SDS-solubilized S5−S6−C-terminus gave pegylation primarily at levels 3 and 4 (lane 4, Figure 5A,B), consistent with additional accessibility of C9, which is located on the lumenal side of the membrane. However, pretreatment with AMS or NEM gave pegylated protein that was at most singly pegylated (lanes 2, 3, 5, and 6, Figure 5A; Table 1). AMS and NEM were able to block C10−C12 and C9−C12, respectively, again consistent with the accessibility of C9 from the lumen, but not from the cytosol (see also Figures 6 and 7). Because S5−S6−C-terminus contains the structural elements of the K^+ channel pore, known to form tetramers in the case of KcsA (*3*), we determined the oligomeric status of this fragment in ER membranes. S5−S6−C-terminus forms only monomers in the membrane, as determined by a sucrose density centrifugation experiment shown in Figure

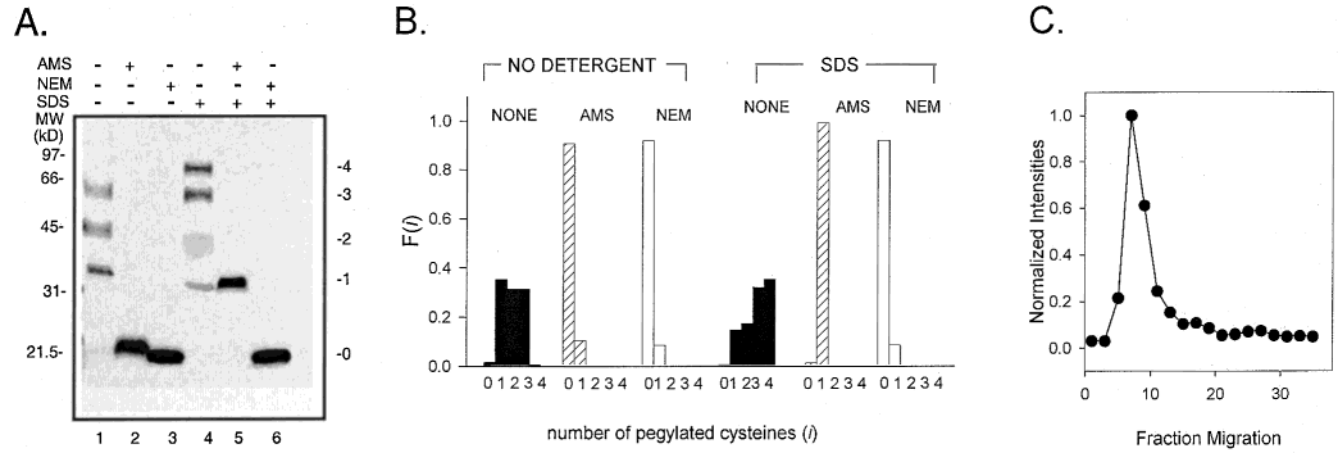

FIGURE 5: Pegylated S5−S6−C-terminus peptide fragment in membranes. (A) S5−S6−C-terminus was translated and labeled with [^{35}S]methionine in a rabbit reticulocyte lysate system containing microsomal membranes, incubated with either no blocking reagent (lanes 1 and 4), AMS (5 mM, lanes 2 and 5), or NEM (20 mM, lanes 3 and 6), and then centrifuged through a sucrose cushion. The vesicles were resuspended in either no detergent (lanes 1−3) or 1% SDS (lanes 4−6) and pegylated. All steps after translation were done at 4 °C. The gels are 10% LDS−NUPAGE Bis-Tris gels with MOPS running buffer. The numbers to the left of the gels are MW standards (kDa); those on the right indicate the number of cysteines (0−4) pegylated. (B) Fraction of S5−S6−C-terminus protein pegylated in no detergent or 1% SDS after preblock with no reagent (black), AMS (hatched), or NEM (white). The fractions of unpegylated and multipegylated protein were calculated as $F(i) = \text{cpm}(i)/\sum\text{cpm}(i)$, $i = 0-i_{max}$), where i is the number of SH pegylated per protein molecule and cpm(i) is the number of counts per minute in the ith bin. The distribution histograms are significantly different for AMS or NEM pretreatment ($p < 0.001$, Komogorov−Smirnov test) compared to control (no pretreatment). The fractional distribution of pegylated S5−S6−C-terminus in SDS is significantly different from binomality ($p < 0.001$, Komogorov−Smirnov test). (C) Sucrose gradients of S5−S6−C-terminus. Protein was translated and labeled with [^{35}S]methionine in a rabbit reticulocyte lysate system containing microsomal membranes, centrifuged through a sucrose cushion, and the vesicles were solubilized in 0.05% $C_{12}M$ and treated as described under Materials and Methods. The fractional migration was calibrated using molecular weight standards (see Materials and Methods). The fractional migration is plotted as cpm normalized to the maximum cpm. Predicted fractional migration for S5−S6−C-terminus as a monomer is fractions 5−7.

5C. The peak fractional migration occurred at fractions 5−7, which corresponds to monomer. We have previously shown that S5−S6−C-terminus is efficiently integrated into the membrane with the correct topology determined for the full-length Kv1.3 channel (*23*). Thus, our results pertain to the monomer fragment and suggest that in monomeric S5−S6−C-terminus cytosolic C10−C12 are available, whereas C9 is available only from the lumen.

The final fragment we analyzed was Kv1.3(T1$^-$), which contains a total of seven native cysteines, including C6−C12. C6−C9 are in transmembrane domains, and C10−C12 are in the cytosolic C terminus. Although Kv1.3(T1$^-$) is missing the first 141 amino acids of the cytosolic N terminus, including the so-called "T1" recognition domain, it is fully functional and has electrophysiological and topological properties virtually identical with those of the full-length wild-type Kv1.3 (*13*, *14*, *23*). As shown in Figure 6A, when Kv1.3(T1$^-$) was pegylated without prior treatment with blocker, four pegylated bands at levels 1−4 (lane 1) were detected in zero detergent, the darkest bands being at levels 2 and 3 (Table 1). We interpret these results as pegylation of C10−12 and partial pegylation of C8. In SDS, pegylation of Kv1.3(T1$^-$) gave a ladder in which all of the protein was pegylated with the darkest bands at levels 5−7 (Figure 6A, lane 4; Table 1; Figure 6B). Pretreatment with AMS gave almost entirely unpegylated protein (level 0) in zero detergent (lane 2) but three pegylated bands at levels 1−3, the major one being at level 2 (lane 5; Table 1; Figure 6B) in SDS. Therefore, all three C-terminal cysteines (C10−C12) and some of C8 were blocked by AMS. Pretreatment with NEM gave only unpegylated protein (level 0) in zero detergent (lane 3), whereas in SDS, Kv1.3(T1$^-$) was present as unpegylated and singly pegylated protein (lane 6; Table 1; Figure 6B). The relative intensities of individual bands in each ladder are shifted toward unpegylated protein in the case of NEM pretreatment, and the distribution histograms are significantly different for no blocker versus AMS or NEM ($p < 0.001$, Kolmogorov−Smirnov test, Figure 6B). These results are consistent with partial blockage of C8 and complete blockage of C10−C12 in both AMS and NEM. Additionally, the three remaining core cysteines, C6, C7, and C9, were partially blocked by NEM, suggesting that in Kv1.3(T1$^-$) C8 and C10−C12 are in the cytosol but that some of the three core cysteines, C6, C7, and C9, are relatively more accessible than the others from lumenal aqueous interfaces.

On the basis of the results obtained with S1, S1−S2−S3, and S5−S6−C-terminus, we hypothesized that the most likely candidate for the least accessible core cysteine is C7. To test this, we mutated C7 in Kv1.3(T1$^-$). As shown in Figure 6C,D and Table 1, elimination of C7 produces protein that has at most six pegylated cysteines in SDS with no preblock and at most singly pegylated cysteines following NEM pretreatment, suggesting that C7 is accessible to NEM and that C6, C8, and C9 are only partially accessible.

The truncated Kv1.3(T1$^-$) is less efficient at forming tetramers than full-length Kv1.3 (*14*, *27*). Two hours of translation in membrane vesicles gave maximal protein for a given amount of cRNA but no tetramer (Figure 6E). However, after 16 h, substantial amounts of tetramer were detected (data not shown). Thus, when Kv1.3(T1$^-$) or Kv1.3(T1$^-$)/C7$^-$ is translated for 2 h and then pegylated in either the absence of detergent or the presence of SDS, the results reflect availability of cysteines in the monomer. However, 40 h post-translation in vivo, Kv1.3(T1$^-$) assembles to give functional channels in *Xenopus* oocytes (Figure 6F).

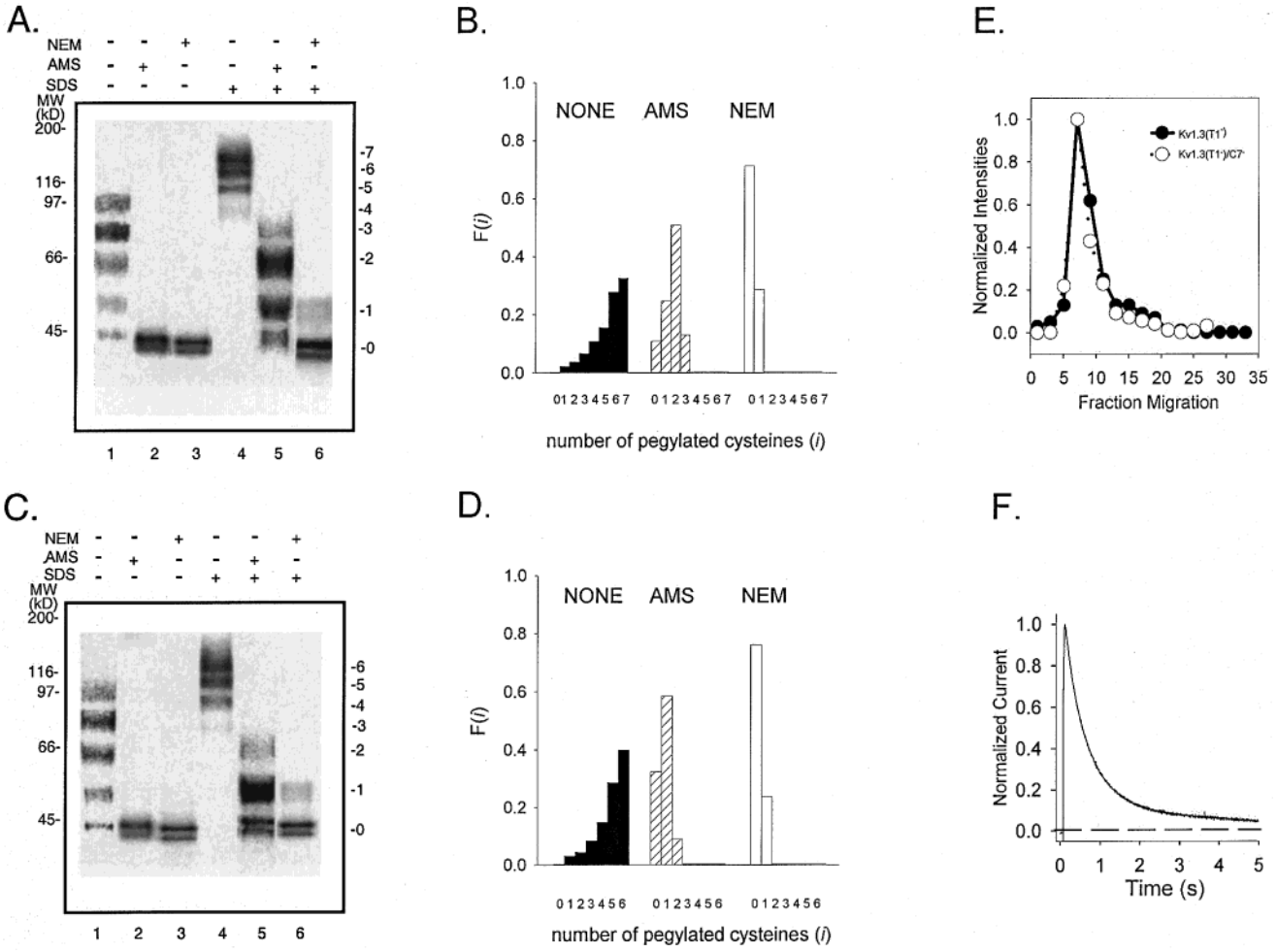

FIGURE 6: Pegylated Kv1.3(T1$^-$) in membranes. (A) Kv1.3(T1$^-$) was translated and labeled with [^{35}S]methionine in a rabbit reticulocyte lysate system containing microsomal membranes, incubated with no reagent (lanes 1 and 4), AMS (lanes 2 and 5), or NEM (lanes 3 and 6), then centrifuged through a sucrose cushion. The vesicles were resuspended in either no detergent (lanes 1−3) or 1% SDS (lanes 4−6) and pegylated. All steps after translation were done at 4 °C. The gels are 4−12% LDS−NUPAGE Bis-Tris gels with MOPS running buffer. The numbers to the left of the gels are MW standards (kDa); those on the right indicate the number of cysteines (0−7) pegylated per Kv1.3(T1$^-$). (B) Fraction of total Kv1.3(T1$^-$) protein pegylated in 1% SDS with the indicated number of MAL-PEG per translated Kv1.3 preblocked with no reagent (black), AMS (hatched), or NEM (white). The fractions of unpegylated and multipegylated protein were calculated as $F(i) = \text{cpm}(i)/\sum\text{cpm}(i)$, $i = 0-i_{max}$), where i is the number of SH pegylated per protein molecule and cpm(i) is the number of counts per minute in the ith bin. (C, D) For Kv1.3(T1$^-$)/C7$^-$, as above in for parts A and B. For both Kv1.3(T1$^-$) and Kv1.3(T1$^-$)/C7$^-$, the distribution histograms are significantly different ($p < 0.001$, Komogorov−Smirnov test) for AMS or NEM pretreatment compared to control (no pretreatment), and the fractional distribution of pegylated protein in SDS is significantly different from binomality ($p < 0.001$, Komogorov−Smirnov test). (E) Sucrose gradients of Kv1.3(T1$^-$)and Kv1.3(T1$^-$)/C7$^-$. Protein was translated and labeled with [^{35}S]methionine in a rabbit reticulocyte lysate system containing microsomal membranes, centrifuged through a sucrose cushion, and the vesicles were solubilized in 0.05% C_{12}M and treated as described under Materials and Methods. The fractional migration was calibrated using molecular weight standards (see Materials and Methods). The fractional migration is plotted as cpm normalized to the maximum cpm. Predicted fractional migrations for Kv1.3(T1$^-$) monomer are fractions 5−7 and for the tetramer, fractions 13−15. (F) *Xenopus* oocytes were injected with cRNA for Kv1.3(T1$^-$), and recordings were made 48 h postinjection. Peak current at +50 mV was measured to give the current trace shown. The dashed line indicates zero current.

Pegylation of Full-Length Kv1.3. Next, we investigated the accessibility of residues in full-length Kv1.3, which contains 12 native cysteines, has been fully characterized electrophysiologically in oocytes (*13*, *14*, *29*), and forms almost exclusively tetramers in the ER membrane within 2 h at 30 °C (*22*; Figure 7). Full-length Kv1.3 was translated in vesicles and either pegylated directly in zero detergent or in SDS or first treated with blocker, either AMS or NEM, and then pegylated in zero detergent or in SDS.

According to the results shown in Figure 7B, in the absence of detergent no unpegylated protein remained and a diffuse ladder could be discerned (lane 2), but not quantitated, beyond four of the cytosolic cysteines (C1−C5, C8, and C10−C12). Pretreatment with AMS or NEM led to only unpegylated protein (lanes 3 and 4). In SDS, pegylation was more robust, yielding neither unpegylated Kv1.3 nor minority labeling, but rather most cysteines (*10*−*12*) were pegylated (lane 5). In this molecular weight range it is difficult to resolve individual bands, especially as this is a gradient gel. Pretreatment with AMS or NEM shifts the majority of pegylated species from 10 to 12 MAL-PEG/Kv1.3 to ≤3 (darkest band is level 3, lane 6, Figure 7B; Table 2) or ≤2 (darkest band is level 1, lane 7, Figure 7B; Table 2), respectively. Both AMS and NEM lead to a significant decrease of pegylated protein (bands appear at levels 1 and 0, lanes 6 and 7). NEM produces more blockage than AMS, consistent with NEM's ability to block lumenal as well as cytosolic sites. A plausible, yet equivocal,

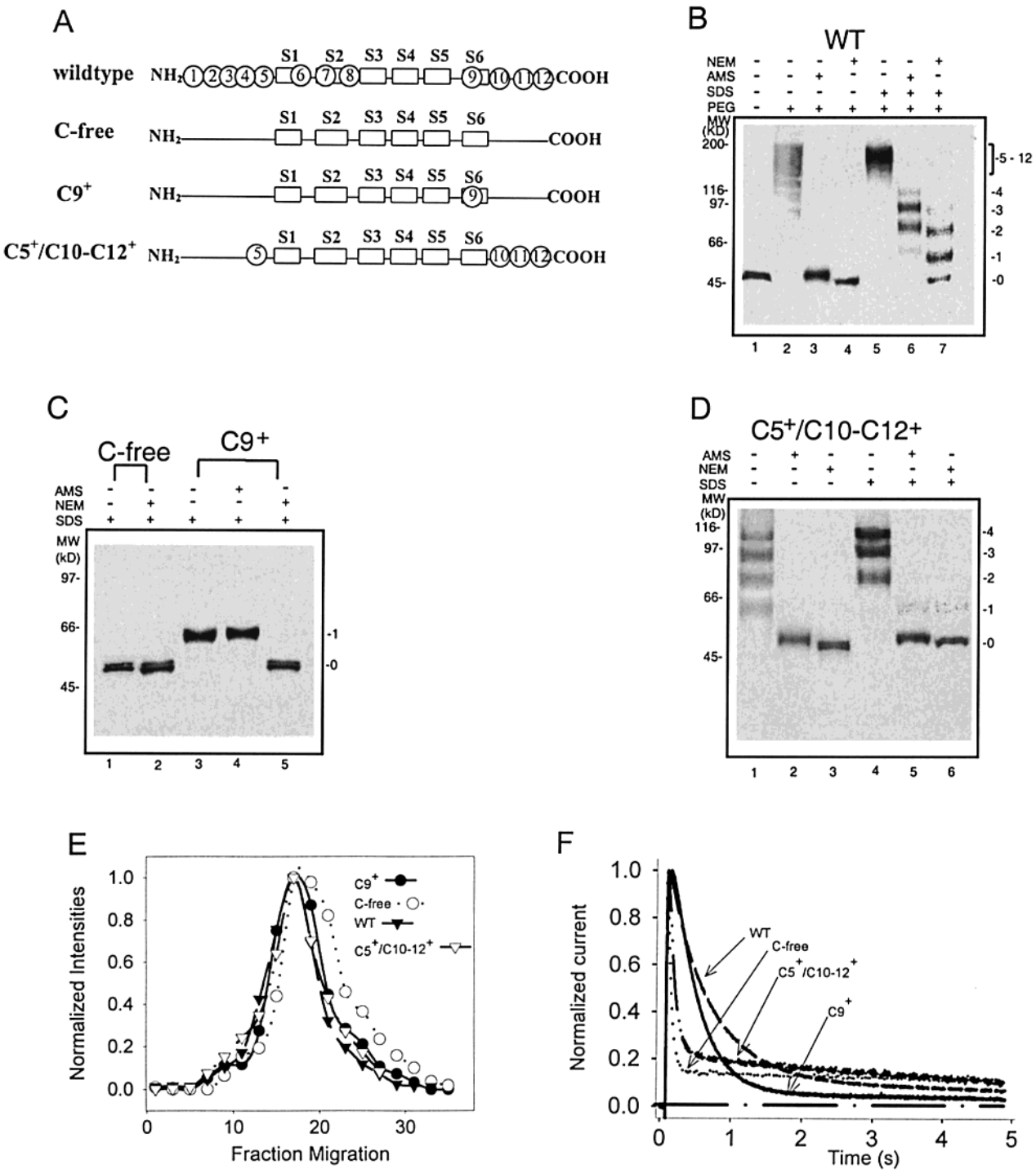

FIGURE 7: Pegylated full-length Kv1.3. Four full-length constructs were characterized by pegylation, fractional migration in a sucrose gradient, and electrophysiology. The constructs are wild type (WT), cysteine-free (C-free), cysteine-free/C9$^+$ (C9$^+$), and cysteine-free containing C5, C10−C12 (C5$^+$/C10−C12$^+$). (A) Schematic representation of the four constructs. Only native cysteines are present and are indicated by encircled C1−C12. (B) WT was translated with membranes, pretreated with no blocker, AMS, or NEM, and centrifuged through a sucrose cushion. The vesicles were resuspended in either no detergent (lanes 1−4) or 1% SDS (lanes 5−7) and pegylated. (C, D) In separate translations, C-free, C9$^+$, and C5$^+$/C10−C12$^+$ were generated in membranes, centrifuged, and resuspended in no detergent (D, lanes 1−3) or in 1% SDS (C, lanes 1−5; D, lanes 4−6), pretreated with no blocker, AMS, or NEM and pegylated. All incubations after translation were done at 4 °C. All gels were 4−12% LDS−NUPAGE Bis-Tris gels using a MOPS running buffer. The fractional distribution of pegylated for WT and C5$^+$/C10−C12$^+$ in SDS is significantly different from binomality ($p < 0.001$, Komogorov−Smirnov test). (E) Sucrose gradients of full-length Kv1.3. Protein was translated and labeled with [^{35}S]methionine in a rabbit reticulocyte lysate system containing microsomal membranes, centrifuged through a sucrose cushion, and the vesicles were solubilized in 0.05% C_{12}M and treated as described under Materials and Methods. The fractional migration was plotted and calibrated as described above. Predicted fractional migrations for Kv1.3 monomer are fractions 5−7 and for the tetramer, fractions 17−19. (F) *Xenopus* oocytes were injected with cRNA for Kv1.3, and recordings were made 24−48 h postinjection. Peak current at +50 mV was measured to give the current trace shown. For clarity, currents are normalized. All current amplitudes ranged between 5 and 10 μA. The inactivation time constants were 613, 95, 388, and 113 ms, respectively, for WT, C-free, C9$^+$, and C5$^+$/C10−C12$^+$. The absence of C9 increases the inactivation time constant, an observation also reported for *Shaker* mutants (*55*). Zero current is indicated by the — · — line.

Table 2[a]

			n						
contruct	detergent	blocker	1	2	3	4	5	6	7−12
WT			0.01	0.04	0.09	0.18	0.30	0.39	**[b]
		AMS	**	**	**	**	**	**	**
		NEM	**	**	**	**	**	**	**

			n				
	detergent	blocker	1	2	3	4	5−12
WT	SDS		**	**	**	**	1.0
		AMS	0.10	0.31	0.37	0.22	**
		NEM	0.33	0.37	0.30	**	**

[a] Data were obtained by PhosphorImager detection of the gel, not necessarily visible in a 16−30 h exposed autoradiogram. Each entry is the fraction of pegylated protein with *n* pegylated cysteines, calculated as $F(n) = \text{cpm}(n)/\Sigma\text{cpm}(n)$, where $n = 1$ to n_{max}. [b] Double asterisks indicate cpm are less than background cpm.

assignment would be that C6, C7, partially C8, and C9 account for the 3.5 pegylated bands in AMS-pretreated SDS pegylation (lane 6), consistent with results for Kv1.3($T1^-$) (Figure 6) and those described below for other full-length constructs. Further assignment cannot be made without additional mutations. It is possible that the inability to label/block some cysteines in the absence of detergent, perhaps including some in the cytosol, is due to the reactivity as well as the accessibility of the residue. The latter possibility may reflect the oligomeric state of protein (see below).

Given the complexity of a 12-cysteine Kv1.3, we mutated all of the native cysteines to create a cysteine-free Kv1.3 (C-free) for further investigation and selective placement of cysteines. C-free Kv1.3 predominantly forms tetramers (Figure 7E), is functional (Figure 7F), and is not pegylated (Figure 7C). Substitution of C9 into the cysteine-free Kv1.3 ($C9^+$) also forms mostly tetramers (Figure 7E), is functional (Figure 7F), and yields one pegylated band (Figure 7C, lanes 3 and 4), which is blocked by NEM but not by AMS (Figure 7C, lanes 5 and 4, respectively). Upon reinsertion of C5 and C10−C12 in the cysteine-free, full-length Kv1.3 ($C5^+$/C10−$C12^+$), tetramers are primarily formed in ER membranes (Figure 7E), the channels are functional (Figure 7F), and all four cysteines are pegylated both in the absence of detergent and in SDS (Figure 7D, lanes 1 and 4; Table 1). Moreover, pegylation of all four cysteines is blocked by AMS or NEM, as indicated by Figure 7D, lanes 2, 3, 5, and 6. These results indicate that C5 and C10−C12 are accessible in the cytosol in the intact tetramer.

Application of Pegylation To Test Putative Protein−Protein Interfaces. Can this approach be used to tell us about putative protein−protein interfaces? To address this issue we chose the T1 recognition domain as a target. Kv subfamilies contain a highly conserved cytosolic N terminus that constitutes a subfamily-specific recognition domain (*30*−*32*). A crystal structure of the T1 domain of a *Shaker*-subfamily Kv1.1a was determined at 1.55 Å resolution (*5*), for *Shaker* itself (*6*), and for Kv1.2 (*7*). In each case, the tetrameric structure surrounds a narrow pore. Each T1 subunit buries 940 Å^2, or 20% of its solvent-accessible surface area, at its two subunit interfaces. Side chains of 15 residues are involved in polar intersubunit interactions and are highly conserved in Kv channels in a subfamily-specific manner. The region crystallized is virtually identical to the T1 region of Kv1.3. On the basis of the T1 crystal structure, we looked for residue pairs that are within 2.4−6 Å of each other at the T1−T1 interface. If the residues are truly this close within the channel tetramer in the ER membrane, then they should be relatively less accessible to pegylation in the absence of detergent.

We chose two pairs of residues: R118/D126 and R62/E64. Each pair was mutated to cysteines in separate constructs (Figure 8A). As a control, we used $C5^+$/C10−$C12^+$, which contains one N-terminal cysteine (C5) in T1, not at the T1−T1 interface but facing the cytosol (*5*−*7*). The other three cysteines (C10−C12) are cytosolic and readily available for pegylation (Figures 6 and 7). One pair, R118C/D126C, can be cross-linked to give tetramers using either oxidizing conditions or bifunctional cross-linkers, whereas the other pair, R62C/E64C, and the control, $C5^+$/C10−$C12^+$, cannot be cross-linked (*33*). The cross-linking results with R118C/D126C and R62C/E64C are similar to results reported by Miller and co-workers for the equivalent pairs of engineered *Shaker* cysteines in oocyte membranes under oxidizing conditions (*8*). As a precaution, all samples were kept in the continuous presence of DTT (1−2 mM) and were diluted into solutions pre-degassed with nitrogen to avoid any air oxidation of cysteines to form disulfides. This was confirmed by the absence of multimer formation using LDS−NUPAGE analysis (data not shown).

Each pair forms mostly tetramers (Figure 8C) and is functional in oocytes (Figure 8D). Figure 8B shows that the R118C/D126C pair was less accessible than the R62C/E64C pair, and both pairs of residues were much less accessible than the four cysteines in $C5^+$/C10−$C12^+$. Within 15 min, >20% of the total $C5^+$/C10−$C12^+$ had all four cysteines pegylated and only a small fraction, ≤5% of the total $C5^+$/C10−$C12^+$, remained unpegylated. In contrast, in the same 15-min period, R118C/D126C was ∼45% unpegylated and R62C/E64C was ∼30% unpegylated. In neither case did incubation as long as 3 h pegylate all of the protein, whereas all of $C5^+$/C10−$C12^+$ is at least singly pegylated and the majority is at least triply pegylated.[2] At 15 min, the average probability, *P*, of a cysteine being pegylated (see Materials and Methods) is 0.65 for $C5^+$/C10−$C12^+$ and only 0.34 for R118C/D126C. The probability for R62C/E64C is intermediate, 0.48. The difference between R118C/D126C and R62C/E64C pegylation histograms is highly significant ($p < 0.001$). Our findings indicate that the relative accessibilities of cysteines are $C5^+$/C10−$C12^+ \gg$ R62C/E64C > R118C/D126C. These results agree with the cross-linking results and are consistent with R118C/D126C and R62C/E64C being at a protein−protein interface in the T1 tetrameric structure.

To obviate any ambiguities due to undetected cross-linking between cysteine pairs, we mutated R118 and D126 in separate constructs. Pegylation of these constructs, D126C and R118C, each containing only one cysteine, is shown in Figure 9. After 15 min, only 23% of D126C and 33% of R118C were pegylated in the presence of 20 mM MAL-PEG, whereas a control construct containing one cysteine,

[2] Moreover, R118C/D126C and R62C/E64C also contain transmembrane native cysteines, C6−C9, which are not labeled during the longer 3-h incubation, again demonstrating the integrity of the membrane and the protein. Only the relative amounts of unpegylated, singly pegylated, and doubly pegylated protein change, not the number of pegylated cysteines.

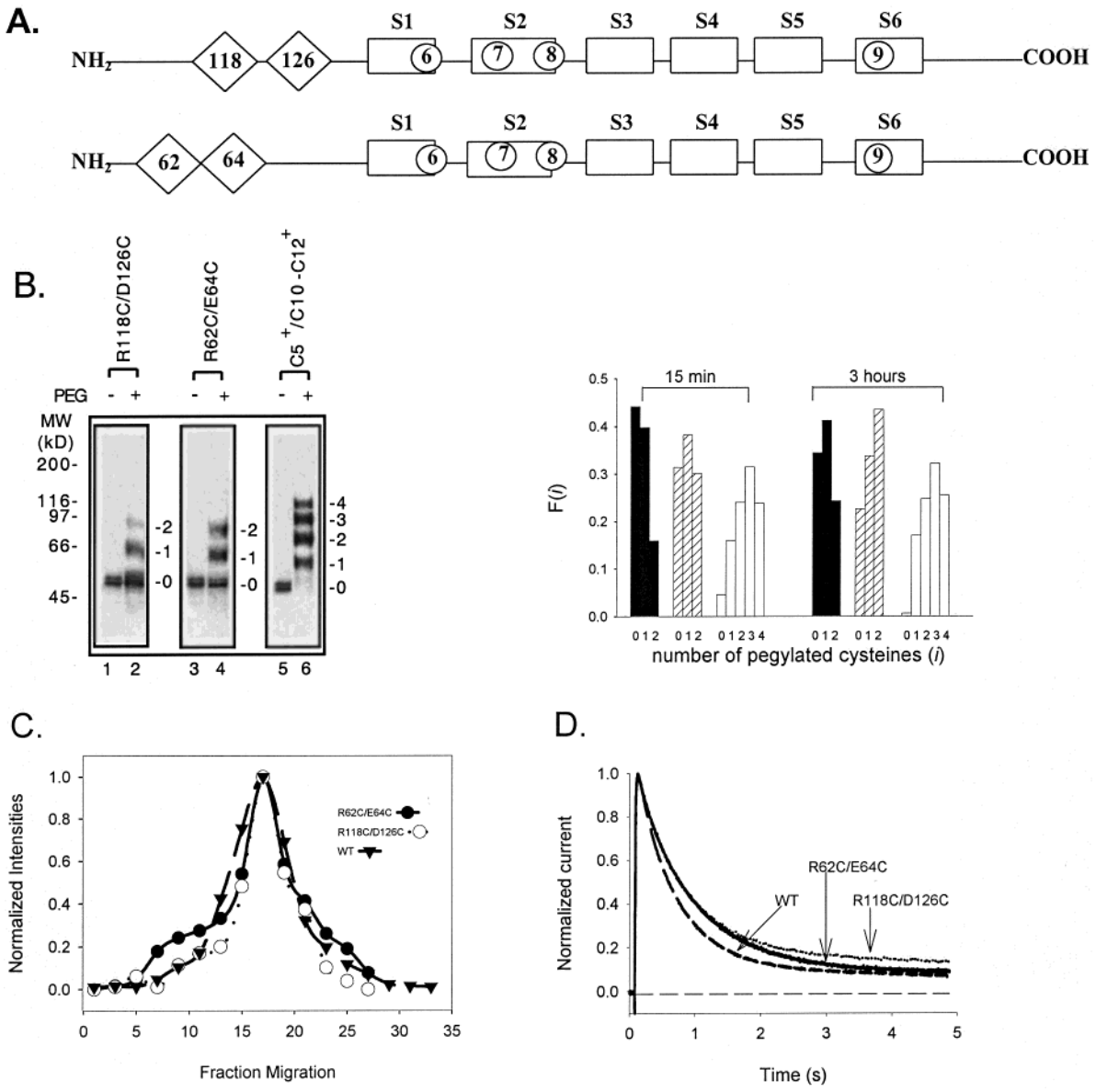

FIGURE 8: Pegylated full-length Kv1.3 containing double mutations in the T1 domain. (A) Schematic representation of R118C/D126C and R62C/E64C. Engineered cysteines, R118C and D126C, R62C and E64C, are shown as diamonds. Native cysteines C6−C9 are shown as circles. (B) R118C/D126C, R62C/E64C, and $C5^+/C10-C12^+$ were generated in membranes, centrifuged through a sucrose cushion, resuspended without detergent, and pegylated. All steps after translation were done at 4 °C. For comparison, $C5^+/C10-C12^+$ was also pegylated. (Left panel) LDS−NUPAGE Bis-Tris gel for 15-min treatment at 4 °C of R118C/D126C (lane 2), R62C/E64C (lane 4), and $C5^+/C10-C12^+$ (lane 6) with MAL-PEG. The gels were 4−12% LDS−NUPAGE Bis-Tris gels with MOPS running buffer. (Right panel) Fractional distribution of pegylated R118C/D126C (black), R62C/E64C (hatched), and $C5^+/C10-C12^+$ (white) at 15 min and 3 h. The difference in pegylation distribution histograms for R118C/D126C and R62C/E64C is highly significant ($p < 0.001$). (C) Sucrose gradients of Kv1.3 containing engineered cysteines. Protein was translated and labeled with [^{35}S]methionine in a rabbit reticulocyte lysate system containing microsomal membranes, centrifuged through a sucrose cushion, and the vesicles were solubilized in 0.05% $C_{12}M$ and treated as described under Materials and Methods. The fractional migration was plotted and calibrated as described above. Predicted fractional migrations for Kv1.3 monomer are fractions 5−7 and for the tetramer, fractions 17−19. (D) *Xenopus* oocytes were injected with cRNA for Kv1.3 containing engineered cysteines, and recordings were made 24−48 h postinjection. Wild-type Kv1.3 (WT) is shown for comparison (data taken from Figure 7). $C5^+/C10-C12^+$ current is shown in Figure 7. Peak current at +50 mV was measured to give the current trace shown. All current amplitudes ranged between 5 and 10 μA. The inactivation time constants were 750, 840, and 613 ms, respectively, for R118C/D126C, R62C/E64C, and WT. Zero current is indicated by the thinner dashed line.

C5, was almost completely pegylated using only 1 mM MAL-PEG. Assuming these cysteines can be completely labeled, as is the case for C6 and C9 (Figures 1, 2, 5, and 7) and considering the 20-fold difference in the concentration of MAL-PEG used to pegylate C5 versus the other mutants, these results indicate that the relative rate constants for pegylation of D126C, R118C, C5 are 1:2:200. As shown in Figures 7D and 8B, C5, a T1 residue that is not at a protein−protein interface (*5*−*7*), is readily available in the cytosol. Thus, the cysteines at the T1−T1 interface have 2 orders of magnitude lower rate constants than the cytosolic-facing T1 residue. As described under Materials and Methods, these results can be used to predict the fraction of cysteines that are unpegylated (P_0) and singly (P_1) and doubly (P_2) pegylated in R118C/D126C. The predicted values are 0.51, 0.41, and 0.08 for P_0, P_1, and P_2, respectively. Moreover, the average probability, P, of a cysteine being pegylated in the R118C/D126C construct is ∼0.30 after 15 min of

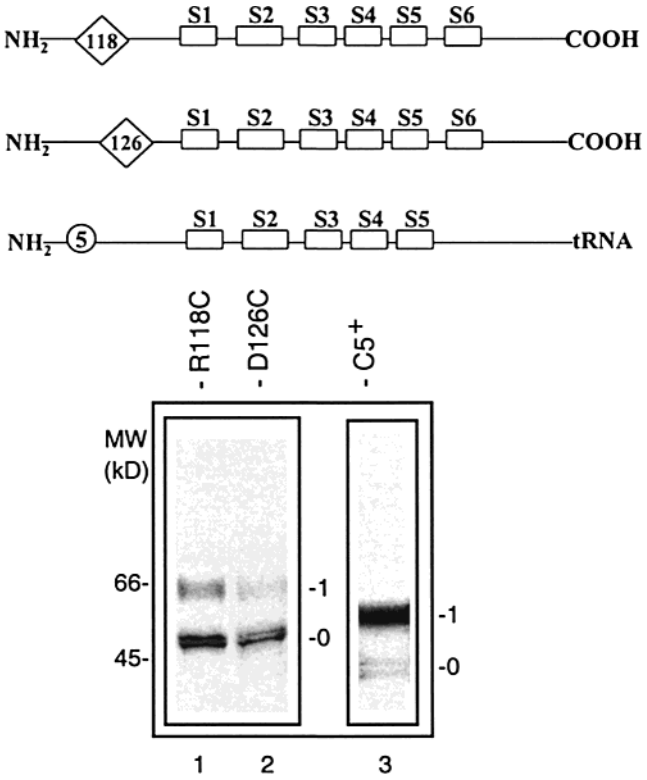

FIGURE 9: Pegylated full-length Kv1.3 containing single mutations in the T1 domain. R118C and D126C were generated in separate translations and pegylated as described in Figure 8. All steps after translation were done at 4 °C. For comparison, $C5^+$ (*Bst*EII-cut and released from tRNA by puromycin; (*33*), containing only C5, was also pegylated. (Bottom panel) LDS−NUPAGE Bis-Tris gel for 15-min treatment at 4 °C of R118C (lane 1), D126C (lane 2), and $C5^+$ (lane 3) with MAL-PEG (20 mM for lanes 1 and 3, 1 mM for lane 3). The gels were 4−12% LDS−NUPAGE Bis-Tris gels with MOPS running buffer.

pegylation, in agreement with the results calculated from the data in Figure 8B. Comparison of these predictions, derived from the singly mutated constructs, with experimental data from the doubly mutated construct provides no evidence for cooperative pegylation between nearby cysteines.

DISCUSSION

Pegylation Method. Pegylation of cysteines is a promising biochemical tool to be used in conjunction with other methods to define membrane protein topology and interfaces involved in oligomeric structures. The strategy of using cysteines to obtain structure/function information for membrane proteins has many precedents, for example, the substituted-cysteine-accessibility method (SCAM; *19*, *28*, *34*), which uses functional manifestations of cysteine modification by methanethiosulfonate derivatives to infer structural information. Yet another example is the use of quaternary amine maleimides with flexible linkers to measure distances between extracellular loop residues and the pore of Kv channels (*35*). More direct structural information is obtained from spectroscopic and biochemical methods in combination with SCAM, which permit detection of functionally silent cysteine modifications (*2*, *4*, *21*, *34*, *36*−*45*). Some of these spectroscopic approaches require large amounts of protein, purification of the protein and/or reconstitution of the protein into lipid, and spectroscopic tools. Biochemical, rather than spectroscopic, methods permit small quantities (picomoles to femtomoles) to be studied using SDS−PAGE techniques. In these cases, conjugated maleimides are bound to cysteines to determine the membrane topology of, for example, human P-glycoprotein (*21*), the peripheral benzodiazepine receptor (*44*), and the α subunit of F_1F_0ATP synthase from *Escherichia coli* (*45*). Furthermore, gel shift assays using small molecular weight SH reagents (e.g., benzophenone-MAL, fluorescein-MAL, and iodoacetylated reagent) have been used to study membrane protein surface accessibility (*46*, *47*). The use of these reagents is limited to small molecular weight proteins, where the resolution on SDS−PAGE permits a detectable gel shift for the cysteine adduct. However, larger polytopic proteins, such as Kv1.3, require a larger mass-tag. PEG (5 kDa) serves this purpose. Recently, an *o*-pyridyl disulfide PEG[3] has been used to study a bacterial surface layer protein layered on a cell wall, specifically to determine which residues are located at the external surface of the S-layer lattice, which are at the intersubunit interface, and which are within the pores (*49*). These approaches detect single cysteines, one at a time. The advantage of a mass-tag method such as ours is that accessibility of multiple cysteines can be evaluated simultaneously, and distribution histograms can be used to understand relative changes in accessibility. The sequential use of blockers (permeant and impermeant) and PEG, and of different detergents (denaturing and non-denaturing) or no detergent, is an effective strategy for determining transmembrane topology and identifying protein−aqueous, protein−lipid, and protein−protein interfaces. Moreover, our approach permits multiple native cysteines to be assessed and dynamic changes in accessibility to be monitored during assembly. In the latter case, multiple reference cysteines can be simultaneously positioned at each interface.

One note of caution is that extrapolation of accessibility measurements in one channel protein, or fragment of the channel, to another should be done judiciously, taking into account that topology is generated through cooperative interactions between multiple topogenic determinants during assembly (*23*). Such determinants may differ for peptide fragments versus full-length channel. Another caveat derives from our limitation to quantitate the fraction of protein that is correctly folded into functional channels in the ER membrane. A final note of caution is that long pegylation times in the absence of detergent can produce high background and aggregation for multi-cysteine constructs. Thus, in the absence of detergent the method works best for short incubation times (1−3 h) and fewer than five cysteines.

Assessment of cysteine accessibility using covalently linked markers depends on the availability of the SH group, its reactivity, and the stability of the adduct. The latter parameter is not an issue in pegylation assays. Rather, the availability and reactivity operationally define accessibility. Factors governing reactivity are the pK_a of the cysteine and the local pH. Availability may be a function of steric exclusion, the protein−protein interface in a folded state of a protein, whether a protein is buried in a lipid membrane at a protein−lipid interface, or whether a protein is free in solution. Among the possible intermolecular protein−protein interactions to consider in our experiments is the oligomeric

[3] *o*-Pyridyl disulfide PEG has also been used recently to locate the constriction in the pore of staphylococcal α-hemolysin (*48*).

state of Kv1.3. Inaccessibility could be due to SH groups that are buried at intersubunit interfaces in a tetramer or oligomeric intermediate. Tetramers of Kv1.3 exist in vitro in microsomal membrane vesicles and are retained in nonionic detergent (*29*; Figures 7 and 8). The Kv1.3 protein distributed in the sucrose gradients represents >90% of the protein in the ER membrane preparations. Therefore, the results of pegylation studies represent the major fraction of Kv1.3 protein in any given sample. Pegylation of full-length Kv1.3 in membrane vesicles in the absence of detergent likely reflects availability of cysteines in the tetramer, whereas pegylation in SDS primarily reflects pegylation of the denatured monomer. AMS and NEM incubations are carried out in the intact membrane vesicle in the absence of detergent, and therefore AMS and NEM react with available cysteines in the tetramer. It is not clear whether all native cysteines in full-length Kv1.3 can be pegylated or blocked with AMS or NEM because in the wild-type channel protein there are more complicated intra- and intersubunit interactions than in the smaller Kv1.3 fragments or mutated full-length channels. Such tertiary and quaternary interactions could alter the availabilities and reactivities of C1−C12.

The presence of a pegylation ladder in the Bis-Tris gels for some multi-cysteine constructs [e.g., S1−S2−S3, S5−S6−C-terminus, Kv1.3(T1$^-$), WT, C5$^+$/C10−C12$^+$] indicates that under the conditions of our experiments, the probability of individual cysteines being pegylated is <1 for all cysteines in the test protein. Additional information can be obtained from analysis of these distributions of pegylated species. For instance, neither the truncated Kv1.3 fragments (Figures 4−6) nor the full-length Kv1.3 constructs (Figure 7) displays a binomial distribution for the number of pegylated cysteines (Figures 4, 6, and 7) in either zero detergent or in SDS (in all cases $p < 0.001$). Binomality assumes that the cysteines in any given protein have identical availability/reactivity and that each is pegylated independently. Because of discrepancies between the observed distributions and the calculated binomial distributions, regardless of whether detergent is present or not, either cooperativity of pegylation or differences in availability/reactivity of the cysteines exist. Our analysis of the data in Figures 8 and 9 provides no evidence for cooperativity in pegylation. Differences in availability/reactivity are expected when the membrane is intact (absence of detergent) as the topologies of C1−C12 are different. Pegylation differences in SDS are more likely to be due to differences in reactivities rather than availabilities because MAL-PEG likely intercalates and equilibrates more readily across a detergent micelle than a membrane bilayer. One possible origin of reactivity differences is suppressed ionization of thiols to thiolate ions (hence, slower reaction with MAL-PEG) of cysteines buried more deeply within the hydrophobic micelle interior. The negative charges of SDS will also suppress ionization.

Topology and Accessibility of Native Cysteines. On the basis of the pegylation results, we have made the following assignments in Kv1.3. C6, near the C-terminal end of S1, faces the lumen at a protein−aqueous interface in fragments S1 and S1−S2−S3 but at a protein−protein or protein−lipid interface in channel-forming species such as Kv1.3(T1$^-$) and wild-type Kv1.3. Such a location is consistent with glycosylation and topological determinations of the S1−S2 loop in Kv1.3(T1$^-$) (*23*). We favor assignment of C7, in the middle of S2, to a protein−protein interface in Kv1.3(T1$^-$), consistent with tryptophan-scanning studies of S2 in *Shaker* (*16*). According to the models for *Shaker* channels (*50*), the corresponding cysteine faces S4 and protrudes into the aqueous vestibule of the "gating pore" or S4 channel (*51*, *52*). Such a location might influence reagent accessibility to C7. For instance, although AMS is negatively charged and therefore might be sensitive to the local potential in the S4 pore (*53*), it is somewhat larger than NEM and may have hindered access to putative crevices (*51*, *52*).

C8, near the C-terminal end of S2, is at a protein−aqueous interface, in equilibrium between exposed and buried states at the cytosolic membrane border. C9, at the N-terminal end of S6, is at an extracellular (lumenal) location. The crystal structure of tetrameric KcsA, which contains a pore region nearly identical to the amino acid sequence of mammalian Kv channels, suggests that C9 is in a groove between S5 and the bottom of the pore helix. The homologous residue in *Shaker* was not labeled with 5 μM tetramethylrhodamine maleimide during a 30-min incubation at 0 °C (*54*). Nevertheless, we were able to modify C9 using 20 mM NEM for 2 h at 4 °C. The lack of labeling in *Shaker* may be due to low concentration or steric hindrance of the bulky tetramethylrhodamine, short exposure time, or the fact that cysteines on the extracellular surface of the plasma membrane are oxidized or otherwise protected. A kinetic analysis of modification rates should provide more insight into the accessibility of C9.

Pegylation studies of S5−S6−C-terminus, Kv1.3(T1$^-$), and full-length C5$^+$/C10−C12$^+$ suggest that the C-terminal cysteines, C10−C12, are in the cytosol at a protein−aqueous interface. Whereas the first two constructs exist as monomers in our pegylation studies, the latter one, full-length C5$^+$/C10−C12$^+$, exists as a tetramer. Yet, in both cases, C10−C12 are available and sufficiently reactive for labeling by MAL-PEG.

In contrast, the N-terminal cysteines C1−C5, although also in the cytosol (*23*), are not all available for pegylation. In full-length tetrameric channels, we only know that C5 is accessible. The crystal structure of the T1 domain (*5*−*7*) predicts that C5 is exposed to the cytosol and should be pegylated. The N-terminal region containing C1−C4 was not included in the peptide used in the crystal structure determination, so we cannot speculate about the ability of C1−C4 to be pegylated. However, membrane-targeting studies (*23*) suggest that the N terminus of Kv1.3 monomers may already exist in a folded state, which could include C1−C4.

The availability and reactivity of cysteines may depend on whether the protein is monomeric or multimeric. Some residues may never be buried at protein−protein interfaces, whereas others may become buried or uncovered as assembly proceeds. Nonetheless, changes in availability and reactivity may accompany tetramerization and, therefore, may be manifest as time-dependent pegylation of Kv1.3. Future studies of Kv1.3 containing engineered cysteines will address these issues. In the meantime, we have studied one possibility of putative inaccessibility, that of the N-terminal cytosolic T1−T1 interface. In the intact, detergent-free system, folded T1 residues shown to be in close proximity (<3.2 Å) at a protein−protein interface and experimentally cross-linkable into disulfide bonds (*8*, *33*) had much lower rates of

pegylation than cytosolic-facing cysteines, namely, C5 in T1 and C10−C12 in the C terminus (Figures 8 and 9). The number of cysteines pegylated, as well as the relative kinetics of pegylation, can be a useful tool for probing relative topological accessibilities in membrane proteins.

ACKNOWLEDGMENT

We thank Dr. L. Tu and J. Wang for technical assistance and Dr. R. Horn for careful reading of the manuscript and assistance with the statistical analyses.

REFERENCES

1. MacKinnon, R. (1991) *Nature 350*, 232−235.
2. Schulteis, C., Nagaya, N., and Papazian, D. (1996) *Biochemistry 35*, 12133−12140.
3. Doyle, D. A., Cabral, J. M., Pfuetzner, R. A., Kuo, A., Gulbis, J. M., Cohen, S. L., Chait, B. T., and MacKinnon, R. (1998) *Science 280*, 69−76.
4. Perozo, E., Cortes, D. M., and Cuello, L. G. (1998) *Nat. Struct. Biol. 5*, 459−469.
5. Kreusch, A., Pfaffinger, P. J., Stevens, C. F., and Choe, S. (1998) *Nature 392*, 945−948.
6. Bixby, K. A., Nanao, M. H., Shen, N. V., Kreusch, A., Bellamy, H., Pfaffinger, P. J., and Choe, S. (1999) *Nat. Struct. Biol. 6*, 38−43.
7. Minor, D. L., Lin, Y. F., Mobley, B. C., Avelar, A., Jan, Y. N., Jan, L. Y., and Berger, J. M. (2000) *Cell 102*, 657−670.
8. Kobertz, W. R., Williams, C., and Miller, C. (2000) *Biochemistry 39*, 10347−10352.
9. Vandongen, A. M. J., Frech, G. C., Drewe, J. A., Joho, R. H., and Brown, A. M. (1990) *Neuron 4*, 433−443.
10. Hopkins, W. F., Demas, V., and Tempel, B. L. (1994) *J. Neurosci. 14*, 1385−1393.
11. Babila, T., Moscucci, A., Wang, H., Weaver, F. E., and Koren, G. (1994) *Neuron 12*, 615−626.
12. Lee, T. E., Phillipson, L. H., Kuznetsov, A., and Nelson, D. J. (1994) *Biophys. J. 66*, 667−673.
13. Tu., L., Santarelli, V., and Deutsch, C. (1995) *Biophys. J. 68*, 147−156.
14. Tu, L., Santarelli, V., Sheng, Z.-F., Skach, W., Pain, D., and Deutsch, C. (1996) *J. Biol. Chem. 271*, 18904−18911.
15. Kobertz, W. R., and Miller, C. (1999) *Nat. Struct. Biol. 6*, 1122−1125.
16. Monks, S. A., Needleman, D. J., and Miller, C. (1999) *J. Gen. Physiol. 113*, 415−423.
17. Li-Smerin, Y., Hackos, D. H., and Swartz, K. J. (2000) *Neuron 25*, 411−423.
18. Li-Smerin, Y., Hackos, D. H., and Swartz, K. J. (2000) *J. Gen. Physiol. 115*, 33−50.
19. Akabas, M. H., Stauffer, D. A., Xu, M., and Karlin, A. (1992) *Science 258*, 307−310.
20. Akabas, M. H., Kaufmann, C., Archdeacon, P., and Karlin, A. (1994) *Neuron 4*, 919−927.
21. Loo, T. W., and Clarke, D. M. (1998). *J. Biol. Chem. 270*, 843−848.
22. Lu, J., and Deutsch, C. (1999) *Biophys. J. 76*, A76.
23. Tu, L., Wang, J., Helm, A., Skach, W. R., and Deutsch, C. (2000) *Biochemistry 39*, 824−836.
24. Grassetti, D. R., and Murray, J. F., Jr. (1967) *Arch. Biochem. Biophys. 119*, 41−49.
25. Rao, C. R. (1973) in *Linear Statistical Inference and Its Applications*, Wiley, New York.
26. Chahine, M., Chen, L.-Q., Barchi, R. L., Kallen, R. G., and Horn, R. (1992) *J. Mol. Cell Cardiol. 24*, 1231−1236.
27. Sheng, Z., Skach, W., Santarelli, V., and Deutsch, C. (1997) *Biochemistry 36*, 15501−15513.
28. Karlin, A., and Akabas, M. H. (1998) *Methods Enzymology 293*, 123−145.
29. Tu, L., and Deutsch, C. (1999) *Biophys. J. 76*, 2004−2017.
30. Li, M., Jan, Y. N., and Jan, L. Y. (1992) *Science 257*, 1225−1230.
31. Shen, N. V., Chen, X., Boyer, M. M., and Pfaffinger, P. (1993) *Neuron 11*, 67−76.
32. Xu, J., Yu, W., Jan, J. N., Jan, L., and Li, M. (1995) *J. Biol. Chem. 270*, 24761−24768.
33. Lu, J., Robinson, M. R., Edwards, D., and Deutsch, C. (2001) *Biochemistry 40*, 10934−10946.
34. Horn, R. (1998) *Methods Enzymol. 293*, 145−155.
35. Blaustein, R. O., Cole, P. A., Williams, C., and Miller, C. (2000) *Nat. Struct. Biol. 7*, 309−311.
36. Kaback, H. R., Voss, J., and Wu, J. (1997) *Curr. Opin. Struct. Biol. 7*, 537−542.
37. Kaback, H. R., and Wu, J. (1997) *Q. Rev. Biophys. 30*, 333−364.
38. Hubbell, W. L., and Altenbach, C. (1994) in *Site-Directed Spin Labeling of Membrane Proteins*, Oxford University Press, New York.
39. Hubbell, W. L., Mchaourab, H. S., Altenbach, C., and Lietzow, M. A. (1996) *Structure 4*, 779−783.
40. Gross, A., Columbus, L., Hideg, K., Altenbach, C., and Hubbell, W. L. (1999) *Biochemistry 38*, 10324−10335.
41. Arkin, I. T., MacKenzie, K. R., Fisher, L., Aimoto, S., Engelman, D. M., and Smith, S. O. (1996) *Nat. Struct. Biol. 3*, 240−243.
42. Arkin, I. T., Adams, P. D., Brunger, A. T., Aimoto, S., Engelman, D. M., and Smith, S. O. (1997) *J. Membr. Biol. 155*, 199−206.
43. Klein-Seetharaman, J., Hwa, J., Cai, K., Altenbach, C., Hubbell, W. L., and Khorana, H. G. (1999) *Biochemistry 38*, 7938−7944.
44. Joseph-Liauzun, E., Delmas, P., Shire, D., and Ferrara, P. (1998) *J. Biol. Chem. 273*, 2146−2152.
45. Long, J. C., Wang, S., and Vik, S. B. (1998) *J. Biol. Chem. 273*, 16235−16240.
46. Krishnasastry, M., Walker, B., Braha, O., and Bayley, H. (1994) *FEBS Lett. 356*, 66−71.
47. Jones, P. C., Sivaprasadarao, A., Wray, D., and Findlay, J. B. (1996) *Mol. Membr. Biol. 13*, 53−60.
48. Movileanu, L., Cheley, S., Howorka, S., Braha, O., and Bayley, H. (2001) *J. Gen. Physiol. 117*, 239−251.
49. Howorka, S., Sara, M., Wang, Y., Kuen, B., Sleytr, U. B., Lubitz, W., and Bayley, H. (2000) *J. Biol. Chem. 275*, 37876−37886.
50. Durell, S. R., Hao, Y., and Guy, R. (1998) *J. Struct. Biol. 121*, 263−284.
51. Yang, N., George, A. L., and Horn, R. (1996) *Neuron 16*, 113−122.
52. Larsson, H. P., Baker, O. S., Dhillon, D. S., and Isacoff, E. Y. (1996) *Neuron 16*, 387−397.
53. Yang, N., George, A. L. J., and Horn, R. (1997) *Biophys. J. 73*, 2260−2268.
54. Mannuzzu, L. M., Moronne, M. M., and Isacoff, E. Y. (1996) *Science 271*, 213−216.
55. Boland, L. M., Jurman, M. E., and Yellen, G. (1994) *Biophys. J. 66*, 694−699.

BI0107647